P-ISSN: 2304-3075; E-ISSN: 2305-4360
International Journal of Veterinary Science
www.ijvets.com; editor@ijvets.com

Research Article https://doi.org/10.47278/journal.ijvs/2024.201

In Vivo Modelling of Metastatic Ovarian Cancer in Wistar Rats Induced by a Carcinogen 7,1 dimethylbenz[a]anthracene

Fara V Diah [1,2], Wawaimuli Arozal [3*], Deni Noviana [4], Andrijono [5], Haryanto Winarto [5], Puspita E Wuyung [6], Vetnizah Juniantito [7], Revina T Putri [8] and Catherine B Ro [9]

[1]Doctoral Program in Medical Sciences, Faculty of Medicine Universitas Indonesia, Jakarta, Indonesia
[2]Department of Obstetrics and Gynecology, Syarif Hidayatullah State Islamic University Jakarta, Jakarta, Indonesia
[3]Department of Pharmacology and Therapeutics, Faculty of Medicine Universitas Indonesia, Jakarta, Indonesia
[4]Faculty of Veterinary Medicine, Bogor Agricultural University, Bogor, Indonesia
[5]Department of Obstetrics and Gynecology, Faculty of Medicine, Universitas Indonesia, Dr. Cipto Mangunkusumo General Hospital, Jakarta, Indonesia
[6]Department of Pathological Anatomy, Faculty of Medicine Universitas Indonesia, Jakarta, Indonesia
[7]Division of Pathology, School of Veterinary Medicine and Biomedical Sciences, Bogor Agricultural University, Bogor, Indonesia
[8]Bachelor in Medicine Program, Faculty of Medicine, Universitas Indonesia, Jakarta, Indonesia
[9]Bachelor in Medicine Program, Faculty of Medicine, Universitas Gadjah Mada, Yogyakarta, Indonesia
***Corresponding author:** wawaimuli@gmail.com; wawaimuli.arozal@ui.ac.id

Article History: 24-488 Received: 26-Apr-24 Revised: 31-May-24 Accepted: 10-Jun-24 Online First: 04-Jul-24

ABSTRACT

Ovarian carcinoma is the second leading cause of death in gynecological cancers after cervical cancer in the world. The use of animal models in testing epithelial ovarian cancer therapy is still necessary, given that the treatment of epithelial ovarian cancer is still not optimal. This study aims to explore the morphologic features and tumor spreading of ovarian cancer in 24-28 weeks of female Wistar rats induced with 2cm silk-coated containing 2mg of 7,1 dimethylbenz[a]anthracene (DMBA). We also measured the systemic toxicity of DMBA implantation on female Wistar rats by assessing the liver and kidney function. Twelve Wistar rats were divided into two groups, sham, and DMBA groups. We analyzed the macroscopic features of the ovarian tumor using ultrasonography to assess ovarian volume, weight, and perimeter. We also analyzed the ovarian tissue's histopathology and the metastatic findings. In addition, we also checked the liver and kidney functions. After 28 weeks of DMBA implantation, the DMBA group showed significant differences in volume, weight, and perimeter between the right ovaries implanted with DMBA compared to the left ovaries in the same group and sham group. All histopathological findings of ovarian cancer in rats induced with DMBA in this experiment were of the serous carcinoma type. Macroscopic and microscopic findings showed cancer spread to the liver, intestines, and lungs, similar to the human pattern of metastasis. Finally, DMBA implantation caused an increase in AST levels along with increased urea and creatinine levels compared to sham rats.

Key words: Animal model, DMBA, Metastases, Ovarian cancer, Ultrasonography

INTRODUCTION

Ovarian cancer is one of the most common causes of death in gynecological cancers. Data from GLOBOCAN 2020 recorded 313,959 new cases of ovarian cancer, with a death toll reaching 207,252 worldwide (Sung et al. 2021). Ninety percent of ovarian cancers are of the epithelial type (Cho and Shih Ie 2009), where two-thirds of cases are found in advanced stages when the tumor has spread to the peritoneal cavity and upper abdominal organs.

One of the modalities commonly used for ovarian cancer screening is transvaginal ultrasonography (TVU). The purpose of TVU is to visualize both ovaries in longitudinal and transverse planes and to calculate volume using the prolate ellipsoid formula (Campbell and Gentry - Maharaj 2018). USG examination can assist

Cite This Article as: Diah FV, Arozal W, Noviana D, Andrijono, Winarto H, Wuyung PE, Juniantito V, Putri RT and Ro CB, 2025. In Vivo modelling of metastatic ovarian cancer in Wistar rats induced by a carcinogen 7,1 dimethylbenz[a]anthracene. International Journal of Veterinary Science 14(1): 39-47. https://doi.org/10.47278/journal.ijvs/2024.201

clinicians in determining whether pathological findings in the ovaries indicate benign or malignant conditions.However, the diagnosis is often made when the cancer has already metastasized extensively. Due to the absence of physical barriers in the peritoneal cavity, ovarian cancer typically exhibits extensive metastasis in the distal intraperitoneal areas, leading to increased morbidity and mortality (Gui and Bivona 2022).

The nonspecific symptoms of ovarian cancer make early detection difficult, resulting in most cases found at advanced stages. Therefore, the discovery of appropriate and optimal therapeutic modalities for ovarian cancer plays a crucial role. The use of animal models holds significant potential in facilitating the development of better methods for early detection and treatment of ovarian cancer. Animal models are being developed accurately to represent the cellular and molecular changes of human ovarian cancer and are expected to depict the biological characteristics of human ovarian cancer (Louisa 2019). Several animal models can demonstrate ovarian cancer either spontaneously or through external manipulation. Some examples of animal models that can show the spontaneous development of ovarian cancer are hens, some strains of mice, and monkeys. However, the low incidence of spontaneous ovarian cancer and the long time required for its occurrence renders these animal models impractical for ovarian cancer experimental research, so animal models used in many studies usually stem from external manipulation (Vanderhyden et al. 2003). The use of rats as experimental animals is based on the similarity of responses in rats and humans to exposure to toxic substances (carcinogens) and the similarity of the rat and human genomes (Rämer et al. 2011).

Additionally, rats are commonly used as research models because they are cheaper, easier to handle and monitor, and have simpler ethical processes (Anisimov et al. 2005). Sprague Dawley (SD) and Han Wistar (HW) rats are the two most commonly used rat species in research in Europe and America, with Han Wistar rats being most frequently chosen due to their advantages of longer lifespan and lower tumor burden (Taylor and Mowat 2020). Wistar rats have smaller body sizes compared to SD rats, making them easier to handle (McCormick 2017). Female reproductive tract tumors are also more frequently found in HW rats than in SD rats, except for benign and malignant granular cell tumors, which are only found in SD rats (Taylor and Mowat 2020).

Animal models of ovarian cancer can be created through several methods, such as induction by carcinogens, stimulation by steroid hormones, and genetic engineering. 7,12- dimethylbenz(a)anthracene (DMBA) is one of the carcinogens capable of inducing cancer growth in experimental animals. DMBA is a fat-soluble compound and thus often accumulates in the adipose tissues, especially in breast adipose tissue (Rengarajan et al. 2015). DMBA promotes carcinogenic mutations by forming DNA adducts that play a role in mutagenesis and carcinogenesis. DMBA metabolism causes DNA damage that affects the growth of regulatory genes, leading to uncontrolled growth (Tan et al. 2006). DMBA causes ovarian stromal damage, resulting in various types of ovarian cancer, such as epithelial, sarcoma, granular, and others (Huang et al. 2012). DMBA can cause organ damage, especially to the kidneys and liver. The liver is a major organ metabolizing chemical compounds entering the body. DMBA metabolism, which produces carcinogenic metabolites and ROS, is vital in liver function damage. The kidneys are essential organs responsible for excreting toxic waste products of metabolism. Thus, they cannot escape from the toxic effects of DMBA metabolites. Research examining the effects of DMBA and Aegle marmelos on breast cancer found that DMBA induction led to liver and kidney degeneration characterized by increased serum bilirubin, AST, ALT, ALP, urea, uric acid, and creatinine levels in the experimental group induced with DMBA compared to the control group (Akhouri et al. 2020).

Due to the limited research on metastasis in animal models, we utilized the DMBA-induced Wistar rats model to observe tumor growth with ultrasound and macroscopic evaluation and assess organ metastasis, histopathological characteristics, and liver and kidney function. Ultimately, this study demonstrated that 28-week-old female Wistar rats induced with DMBA successfully developed ovarian cancer with serous carcinoma histological features.

MATERIALS AND METHODS

Animal ethics

The Institutional Animal Care and Use Committee of Universitas Indonesia approved this study (approval number: KET-148/UN2.F1/ETIK/PPM.00.02/2023).

Materials

The materials used in this research were DMBA (purchased at Sigma-Aldrich, USA), ketamine (purchased from CV Cahaya Rahayu) and xylazine purchased from CV Tekad Mandiri Citra, Jakarta, Indonesia.

Animal experiment

The rats used in this study were healthy female Wistar rats aged 6-8 weeks obtained from an animal research breeding facility (Biofarma, Bandung, Indonesia). They were housed at a temperature of 25±2°C, humidity of 65±10%, and a 12-h/12-h light/dark cycle and fed with standard pellets. We divided the test animal groups in this study into the sham group and the DMBA induction group, each group consisting of six rats.

DMBA implantation procedure

Surgery was performed under intraperitoneal anesthesia using ketamine (75mg/kg BW) and xylazine (8.8mg/kg BW). The procedure was conducted in the retroperitoneal area, and adipose tissue was detached from the ovary (Fig. 1). Two milligrams of DMBA were heated for 10min at a temperature of 124ºC, then coated onto two centimeters of silk suture 3-0, which was subsequently implanted directly into the ovarian tissue. Finally, the incision wound was closed. The time required from the implantation process to tumor mass formation was at least 20 weeks.

Ultrasonography examination procedure

Female Wistar rats induced with ovarian cancer undergo ultrasonography examination at weeks 24 and 28 to observe the development and growth of ovarian cancer. The rats were intraperitoneally anesthetized with ketamine (75mg/kg BW) and xylazine (8.8mg/kg BW). Their peritoneal fur was shaved and cleaned, and the gel was applied to the peritoneal area to aid the ultrasonography

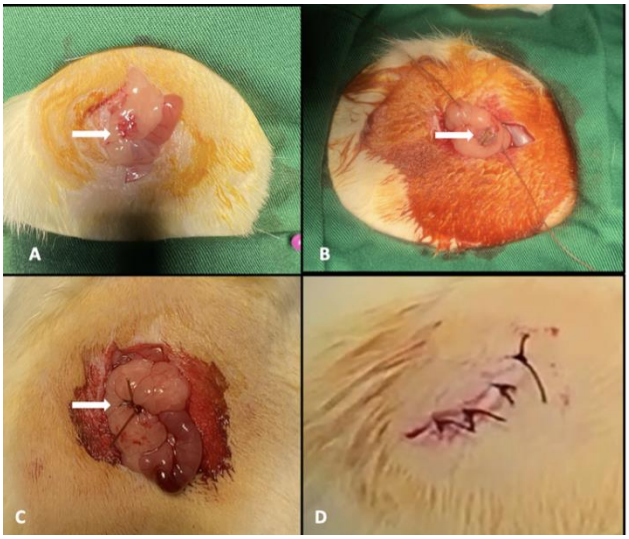

Fig. 1: Surgical approach of the silk-coated implant of DMBA in Rats. A) Incision of retroperitoneal tissue, B) Implantation of chromic 3.0 coated by DMBA in rat right ovary and sutured, and C) Ovary was covered with bursa (arrows).

examination process. Ultrasonography examination on the rat ovaries was performed using a portable ultrasonography Ebit 60 Vet ® (Mega Utama Medica, Indonesia). The sonogram displayed perimeter, length and width data (transversal and longitudinal point of view) using a multi-linear transducer at 50–60MHz frequency. A perimeter was defined by the circumference of the ovary measured by ultrasonography. The formula obtained the calculation of ovarian volume by ultrasonography: V = 0.523 x L x W x H (L = length; W = width; H = height). The actual volume (macroscopic volume) was calculated using the formula: V = 0.5 x L x W2 (L = length; W = width; V = volume). In this study, the parameters to be measured were tumor volume, ovarian weight, and ovarian perimeter.

Macroscopic findings of metastasis to other organs

All of the animals were sedated with ketamine (70mg/kg BW, i.p.) and xylazine (7.0mg/kg BW) before being sacrificed to reduce any pain, suffering, or distress during the experiment. After the rats were sacrificed, abdominal layers were incised, and organ metastasis was evaluated. The metastasis organ was removed after being dissected and examined for histopathology.

Tissue preparation and analysis for histopathology

The ovaries of the rats were removed after being dissected, and we weighed them, cut them longitudinally, and examined them for morphology. The 24-48 hours fixation of ovarian organs in 10% neutral buffer formalin, routinely processed and embedded in paraffin wax. Sections were made at 5µm, embedded in paraffin, and stained with Hematoxylin and Eosin (H & E). Additionally, pathologists conducted histopathological analysis anonymously.

Liver and kidney function analysis

Blood samples collected from the orbital venous plexus were centrifuged (3,000g) for 20min at 4°C. The serum was extracted and examined for aspartate aminotransferase (AST), alanine transaminase (ALT), creatinine, and urea levels using commercial kits (DiaSys, Indonesia).

Data analysis

All collected data were inputted into SPSS for Mac version 23.0. Data are presented in mean±SD. Unpaired t-tests and Mann-Whitney were applied for statistical analysis with a significant limit (α) of 0.05. The value of $P<0.05$ showed a significant difference between the groups. The graphs and statistical analyses were conducted using GraphPad Prism version 9.0.0.

RESULTS

Ultrasonography analysis of ovarian organs at week 24 and week 28

Ultrasound findings at 24 and 28 weeks were carried out on ovarian rats to see the characteristics of the ovaries. The right ovary was the implanted site of DMBA-coated silk. We could see the development of right and left ovaries on perimeter, area, and volume at 24 and 28 weeks.

Statistical analysis of ovarian perimeter at 24 weeks revealed a significant ($P<0.05$) difference in perimeter of right ovaries between Sham and DMBA group (Table 1; Fig. 2), while there was no difference ($P>0.05$) in perimeter of left ovary between Sham vs DMBA group. Furthermore, the right ovary in the DMBA group showed significantly ($P<0.05$) greater values than the left.

Table 1: Ultrasound Characteristics of Tumor Models

Parameters	Sham (n=7)	DMBA (n=7)
24 weeks		
Perimeter		
Right (cm)	1.60±0.259aA	5.31±1.783bA
Left (cm)	1.79±0.643aA	2.80±0.717aB
Area		
Right (cm^2)	0.141±0.050	1.785±1.579aA
Left (cm^2)	0.167±0.110	0.507± 0.274aB
Volume		
Right (cm^3)	0.036±0.015	1.936±2.631
Left (cm^3)	0.045±0.039	0,246±0.186
28 weeks		
Perimeter	1.6±0.181aA	6.667±2.730bA
Right (cm)	1.28 (0.073)aA	1.874(0.549)aB
Left (cm)		
Area	0.153±0.047aA	3.451±2.558bA
Right (cm^2)	0.107± 0.013aA	0.24±0.149aB
Left (cm^2)		
Volume	0.052± 0.05aA	5.233±5.321bA
Right (cm^3)	0.03±0.011aA	0.117±0.077aB
Left (cm^3)		

Values (mean±SD) bearing different small letters in a row and capital letters in a column under a specific parameter differ significantly ($P<0.05$).

The statistical analysis of ovarian area at 24 weeks in the DMBA group showed significantly ($P<0.05$) greater values for the area of right ovary compared to the left ovary, while there was no difference in area of right and left ovary between sham vs DMBA group (Table 1).

The statistical analysis of ovarian perimeter at 28 weeks revealed a significant difference ($P<0.05$) in the perimeter of right ovaries between the Sham and DMBA group. However, there was no difference in the perimeter of the left ovary between the Sham and DMBA groups. Additionally, we observed that the right ovary in the DMBA group exhibited significantly greater perimeter values than the left ovary ($P<0.05$). Furthermore, the statistical analysis for ovarian area and

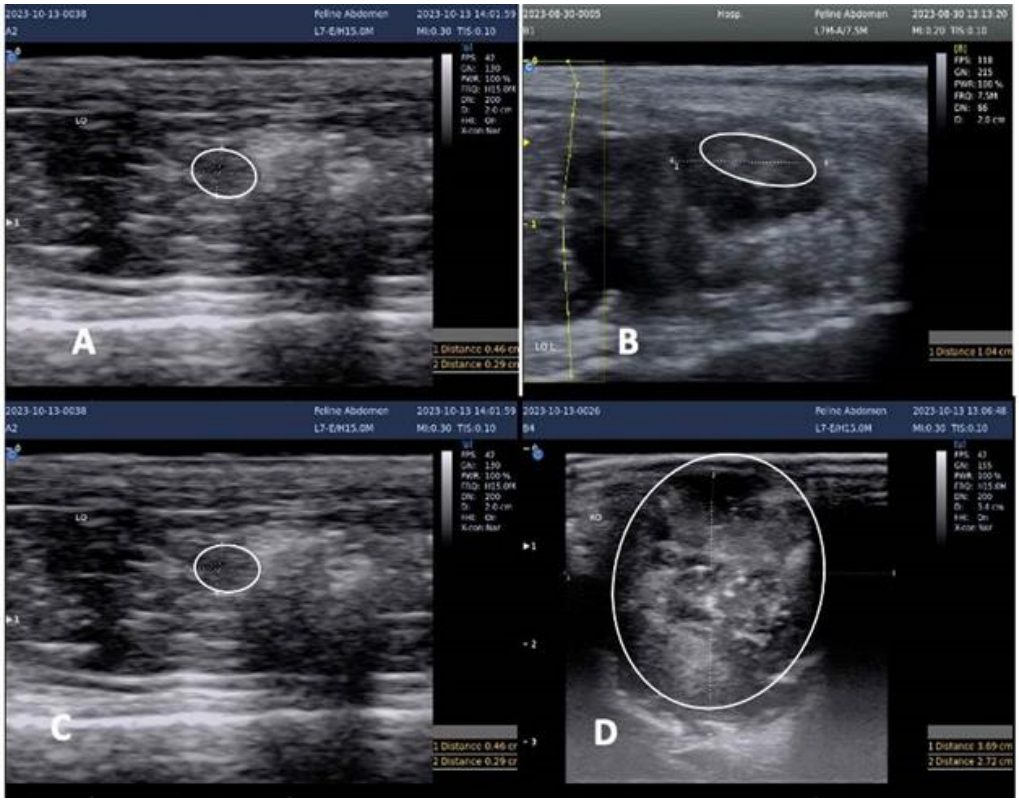

Fig. 2: The ultrasonography of ovaries in Sham and DMBA-treated rats; continuous lines indicated ovaries. A) Ultrasonography of 24 weeks of left ovary rat (normal ovary without implantation), B) Right ovary of implanted DMBA at 24 weeks, C) Normal left ovary of 28 weeks, and D) Right ovary of implanted DMBA at 28 weeks.

volume also revealed a significant (P<0.05) difference in right ovary between the Sham and DMBA groups. In the DMBA group, we found significantly (P<0.05) greater values of area and volume in the right ovary compared to the left ovary (Table 1).

Table 2: Weight and Volume macroscopic of Tumor Models

Ovarian Parameters	Sham (n=7)	DMBA (n=7)
Weight (mg)		
Right	90(40-120)aA	3500 (480-21760)bA
Left	100 (60-140)	120 (120-160)
Volume macroscopic (cm3)		
Right	0.051 (0.028-0.062)aA	1.612 (305.1-14335)bA
Left	0.043(0.028-0.084)	0.030 (0.016-0.061)

Values represent the median (min-max) bearing different small letters in a row and capital letters in a column under a specific parameter differ significantly (P<0.05).

Macroscopic overview and pattern of spreading ovarian cancer

The weight and macroscopic volume of the ovaries after sacrifice can be seen in Table 2. Based on the results of the statistical analysis of the normality test (Kolmogorov-Smirnov test) and homogeneity test (Levene test) with a significance value of homogeneity of 0.200 (P<0.05), it can be assumed that rats' ovary weight and macroscopic volume were not normally distributed and varied heterogeneously. The analysis was continued with Mann-Whitney and obtained a significance value of rat ovary size of 0.003 (P<0.05) and also a significance value of rat ovary macroscopic volume of 0.001 (P<0.05). These results indicate significant differences between the right ovary weight of 3500mg (480-21760) and the right ovary in the sham group. The results also showed that the macroscopic volume of the right ovary of rats implanted by DMBA was significantly increased compared with the right ovary of the sham group. In the 28th week, the sacrifice was performed. Tumor spread in rats that implanted DMBA to intra-abdominal organs such as the liver, lung, and bowels were seen in Fig. 3. Rats also showed involvement of mesentery and ovarian carcinoma on 28 week (Fig. 4).

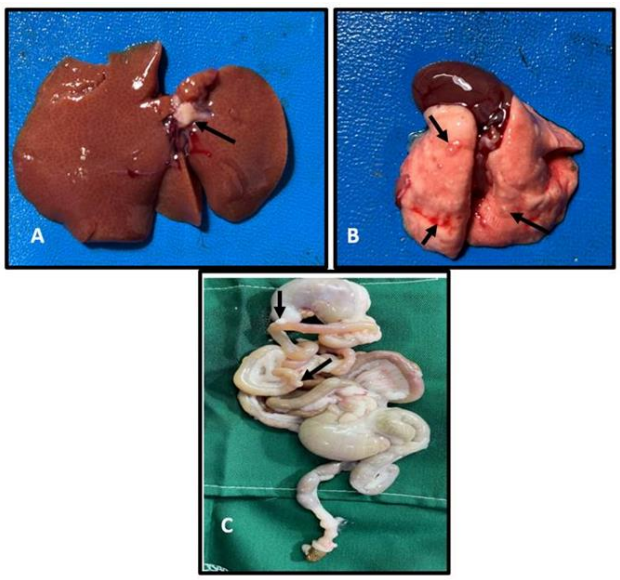

Fig. 3: Macroscopic appearance of metastasized ovarian tumor in DMBA-treated rats. A) Tumor metastasis to the liver (arrows), B) Lung metastasis (arrows), and C) Intestinal serosa metastasis (arrows).

Histopathology of ovaries in the DMBA-treated rats

Using histopathology, we examined tissue morphology in the left and right ovary of sham and DMBA-treated rats. Histopathologically, the ovaries of the sham rats showed no visible abnormalities (Fig. 5).

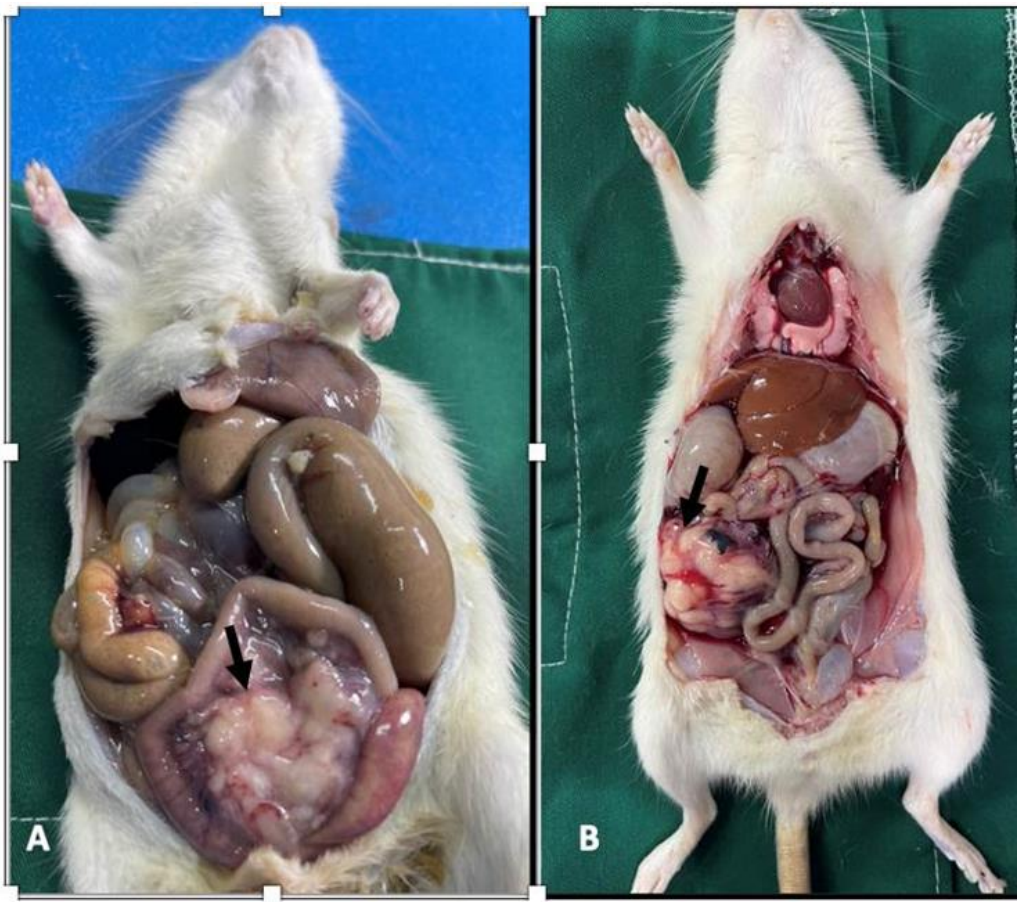

Fig. 4: 28 weeks rat showing A) mass with mesenteric involvement, and B) right ovarian carcinoma.

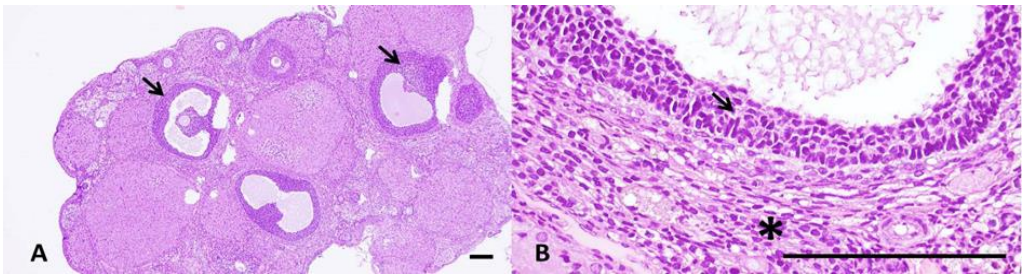

Fig. 5: Photomicrograph of the left ovary after 28 weeks of DMBA treatment in rats. A) Normal left ovary with ovarian follicles (arrows); and B) Normal histology of ovarian follicle epithelia (arrow) and stromal tissue (asterisk). H & E Stain. Bar=100µm.

DMBA-treated rats' ovaries show multifocal to solid formations of atypical cell clusters organized in glandular patterns and creating arboriform papillae (Fig. 6). The papillae that define these tumors are made up of stroma lined with single or numerous layers of cuboidal or columnar epithelial cells. The tumor's glandular shape consists of a reasonably regular gland structure, numerous types of stromal cells, and an incomplete and irregular glandular structure. There were also numerous foci of necrosis and hemorrhages and moderate to severe infiltrations of macrophages and lymphoplasmacytic inflammatory cells throughout the mass (Fig. 6). Mitotic cells are also identified in varied numbers throughout the tumor mass (10-40mitotic cells/2.37mm^2). Tumor cells can be seen in the lumens of lymphatic or microvascular capillaries, indicating lymph vascular invasion of the tumor. Based on the current findings, the results on the right ovary in the 28th week resembled high-grade serous carcinoma (Table 3). Furthermore, histological conformations of tumor metastatic nodules to neighboring tissue and distant organs have been observed in the intestinal serosa, liver, and even the lungs (Fig. 7).

Liver and kidney functions

The liver and kidney functions of the rats with right ovary induced by DMBA were seen in Table 4. Based on the results, the mean of AST in the DMBA group slightly increased but was not significantly different from that of the sham group ($P>0.05$). The levels of ALT, urea, and creatinine in the DMBA group were significantly ($P<0.05$) higher compared to the Sham group (Table 4). These values were clinically not significant even though they statistically showed significant differences.

DISCUSSION

This research has successfully demonstrated that DMBA implantation in the right ovaries of Wistar rats has developed an ovarian cancer model. We found significant differences in ultrasound parameters (the perimeter, area, and volume), ovarian weight, and macroscopic volume in the right rat's ovary between the DMBA group compared with the right ovary in the sham group in 28 weeks. A significant difference was found in the DMBA group comparing right and left ovaries. This result is caused by the carcinogenic effects of DMBA, which can induce carcinogenic mutations

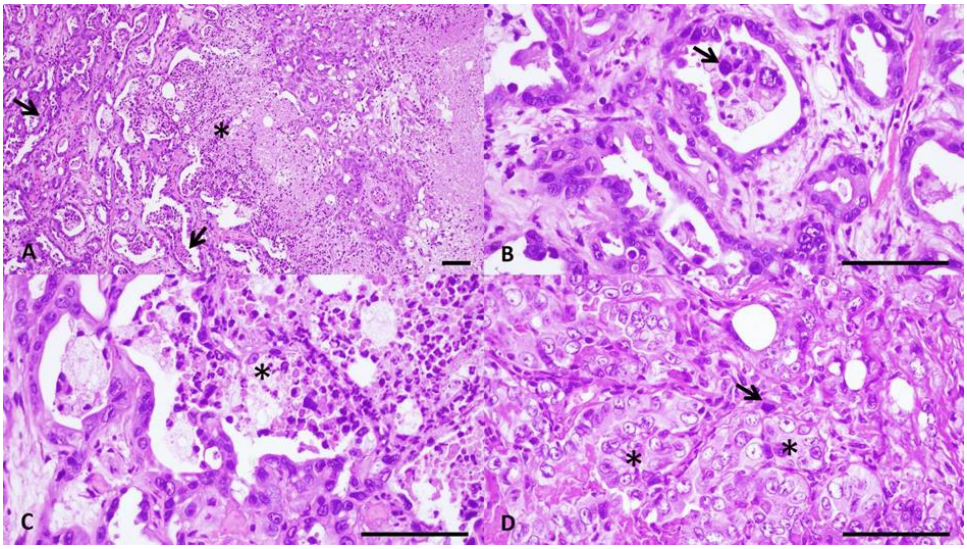

Fig. 6: Histopathology of ovarian serous carcinoma after 28 weeks of DMBA treatment in rats. A) arboriform papillae formations (arrows) along with area of necrosis (asterisk), B) glandular pattern of tumor lined with a single layer or multiple layers of columnar epithelia with small papillary projections into the lumen (arrow), C) area of necrosis characterized by tumor cells with small nuclei (pyknosis), and loss of nuclei (karyolysis), and D) glandular pattern consists of solid arrangement of tumor cells without lumen (asterisks), and atypical mitotic cell (arrow). H & E Stain. Bar=50µm.

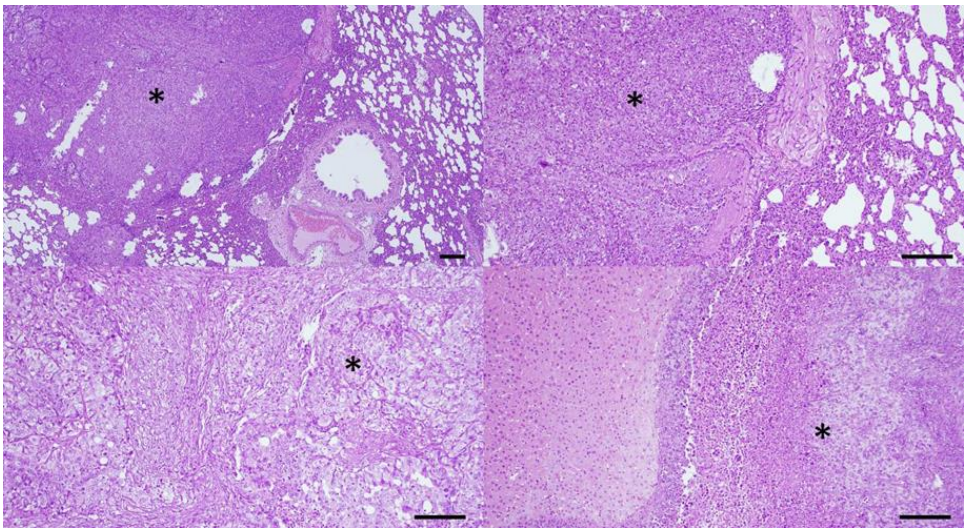

Fig. 7: Photomicrograph of the ovary of a rat induced by DMBA showing A) and B) ovarian tumor metastatic sites in the lungs (asterisks), C) intestinal serosal metastasis (asterisk), and D) metastasis to the liver (asterisk). H & E Stain. Bar=100µm.

Table 3: Histopathology of sham group and DMBA induces carcinoma in each rat

Group	Histopathology
Sham	Normal
DMBA	
No 2	Serous Carcinoma
No 4	Serous Carcinoma
No 5	Serous Carcinoma
No 6	Serous Carcinoma
No 7	Serous Carcinoma
No 9	Serous Carcinoma
No 13	Serous Carcinoma
No 14	Serous Carcinoma

Table 4: Liver and Kidney Function of 28 weeks Ovarian Rats induction by DMBA

Parameters	Sham (n=7)	DMBA (n=7)
AST (IU/L)	24.44±3.32	30.50±7.12
ALT(IU/L)	19.05±3.52a	12.94±2.491b
Urea (mg/L)	24.44±3.32a	39.88±8.625b
Creatinine (mg/L)	0.22±0.139a	0.54±0.254b

Values (mean±SD) bearing different small letters in a row differ significantly ($P<0.05$). AST=Aspartate Aminotransferase; ALT=alanine aminotransferase.

through DNA adduct formation. The incidence of DMBA-induced ovarian cancer varies from 10–45%, primarily due to differences in rat strains, the chemical form of DMBA used, and the route of DMBA administration. DMBA causes damage to ovarian stroma, resulting in various types of ovarian cancer, such as epithelial, sarcoma, granular, and others (Huang et al. 2012).

DMBA is an indirect-acting carcinogen that requires metabolic activation to produce its carcinogenic form. The main activation pathway of DMBA is the bay region dihydrodiol epoxide pathway. DMBA is oxidized by CYP1A1 and microsomal epoxide hydrolase in the liver to form DMBA 3,4-oxide. The enzyme epoxide hydrolase then converts 7,12-DMBA-3,4-oxide to DMBA-3,4 diol. Subsequently, oxidation by CYP promotes the formation of DMBA-3,4-diol-1,2-epoxide, the primary carcinogen that interacts with DNA to form adducts that play a role in mutagenesis and carcinogenesis. Cancer growth and development can occur if mutations occur in tumor suppressor genes or oncogenes (Rengarajan et al. 2015). DMBA metabolism causes DNA damage, affecting the growth of regulatory genes and leading to uncontrolled growth. DMBA is an environmental carcinogen with potent ovotoxic effects on the ovaries, causing a decrease in the number of follicle cells by disrupting folliculogenesis processes, leading to premature ovarian failure. The formation of DMBA-DNA adducts can directly cause follicular atresia. PCR analysis to observe the toxic effects of DMBA on the ovaries showed an increase in the number

of Ddx5 and Foxn3 genes, which promote follicular atresia. Ddx5 acts as a co-activator of estrogen receptors, and its increased expression aims to promote the growth and survival of cancer cells (Sandhiutami et al. 2019).

The genetic origin of cancer metastasis can be explained through two models. The first model is called the seed and soil hypothesis. This hypothesis explains that cancer is genetically heterogeneous, and metastasis arises from clones with genetically acquired metastatic phenotypes, while the clone's genotype determines the metastasis's final location. The second hypothesis states that metastatic cells are not genetically selected clones different from the primary tumor but arise from cells that are genetically identical to the primary tumor (Tan et al. 2006). This hypothesis is consistent with research conducted by Hibbs et al. (2004), who found similar gene expression profiles in 17 primary serous papillary ovarian carcinomas with omental metastasis, and by Israeli et al. (2004), who studied the relationship between the primary tumor of ovarian cancer and intraperitoneal metastasis, where genetic changes were found not only in the primary tumor but also at the metastatic site.

Epithelial ovarian cancer metastasis can occur through three mechanisms: transcoelomic, hematogenous, and lymphatic routes. Transcoelomic metastasis is the most common mechanism in ovarian cancer metastasis. The process of transcoelomic metastasis can be a continuous adaptive behavior or a passive process. When cancer cells detach from their primary site, these cells are believed to metastasize through a passive mechanism influenced by the physiological movement of peritoneal fluid towards the peritoneum and omentum (Lengyel 2010), thereby affecting important organs in the abdomen such as the digestive and genitourinary systems (Tan et al. 2006). Although the anatomy of the peritoneum itself facilitates transcoelomic metastasis, ovarian cancer epithelial cells also exhibit adaptive cellular behavior that leads to metastasis. The mechanism of transcoelomic metastasis begins with the release of tumor cells from their primary site. The process of tumor cell release is complex and involves multiple factors. The mechanism of tumor cell detachment from the primary tumor site is not clear yet, but it is presumed to occur due to changes in cell adhesion conditions. Integrins play a crucial role in cell adhesion to the actin cytoskeleton and extracellular matrix ligands, as well as in cell motility, proliferation, and survival, so changes in integrin expression can lead to the detachment of cells from their primary site. In addition to integrins, tumor cell adhesion is also influenced by plasminogen-activator inhibitor 1, which deactivates tumor cell adhesion and the extracellular matrix and the hepatocyte growth factor. In addition to changes in cell adhesion, metastasis is also associated with the loss of apoptotic cell ability. Increased expression of RAB25, protein B7-H4, MMP, endothelin 1, and decreased expression of E-cadherin prevent apoptosis and anoikis and increase the aggressiveness of cancer cells, leading to cell transformation into malignancy (Tan et al. 2006). These detached cells can take the form of individual cells or form spheroids (aggregated ovarian cancer cells). Both adhere to mesothelial cells lining the peritoneal cavity and invade the submesothelial extracellular matrix (Barbolina 2018).

Based on its origin histologically, ovarian cancer is classified into three major groups: coelomic epithelium (epithelial ovarian cancer), germ cells (germ cell tumors), and mesenchymal (stromal cell tumors) (Eisenhauer et al. 2018). All epithelial ovarian tumors are classified as serous tumors, mucinous tumors, endometrioid tumors, clear cell tumors, Brenner tumors, undifferentiated carcinomas, mixed epithelial tumors (tumors consisting of two or more of the five major epithelial tumor types), peritoneal carcinomas, or serous carcinomas of the undesignated site (Berek et al. 2021). Classification of animals' ovarian tumors does not typically include the serous (low and high grade), endometrioid, clear cell, and mucinous forms that are prognostically significant in their human counterparts. However, in this study, DMBA implantation in the right ovaries of Wistar rats showed histopathological features resembling high-grade serous carcinoma characterized by histological features such as arboriform papillae, glands with irregular shapes, necrotic foci, and lymph vascular invasion. These findings may be due to the location of DMBA implantation on the ovarian surface.

The method of DMBA administration may be one of the factors influencing the histology of ovarian cancer types produced in the Wistar rat model. Intragastric or intravenous DMBA administration shows histological findings of stromal tumors (Tunca et al. 1985). In the group of rats implanted with silk coated with DMBA, histological views of adenocarcinoma (21/37), squamous cell carcinoma (3/37), granulosa tumor cells (3/37), sarcoma (4/37), undifferentiated carcinoma without adenoid features (2/37), benign ovarian tumors (2/37), and malignant teratoma (1/37) were found. Meanwhile, the histological findings found in rats implanted with a cloth soaked in high-purity DMBA were 93.75% adenocarcinoma and sarcoma (6/96). Differences in surgical procedures may cause differences in the histology findings of ovarian cancer. In the group of rats implanted with DMBA-coated cloth, the inside of the ovaries was not intervened, and surgery was only performed on the membrane pouch, allowing the surface cells of the ovaries to be exposed to the carcinogen.

Meanwhile, in the group implanted with DMBA-coated silk, injury to the inside of the ovaries could not be avoided when inserting the layered DMBA-coated silk with a needle that allows the drug to penetrate tissues other than the surface. This study successfully proves that the origin of epithelial ovarian cancer is the surface cells of the ovary, and other types of cancer may originate from the middle layer of the ovary (Huang et al. 2012). Research by de Souza et al. (2023), which used Fischer rats with the DMBA administration method via injection into the ovarian bursa at a dose of 1.25 mg/kg, found that the histopathological results of ovarian cancer formed were serous carcinoma with molecular features similar to low-grade serous ovarian carcinoma.

Apart from the DMBA administration method, several other factors that contribute to different histological findings in rat models are the rat strains used, location of carcinogen implantation, dosage, duration of carcinogen exposure, and the time interval required before tissue collection (Huang et al. 2012). In C57BL6 strain rats receiving daily doses of DMBA via gavage for three weeks, histological features of granulosa cell tumors were found in

71% of the experimental animals after one year (McDermott et al. 2007). Another study observing cancer occurrence in rats with P53 mutations found that 80% of rats implanted with DMBA-coated threads in the ovaries successfully developed ovarian cancer models, with 50% showing adenocarcinoma features after three months (Wang et al. 2008). A study conducted by Crist et al. (2005) found that in rats with DMBA-coated thread implantation in the left ovary, 39% (9/23) of the rats exhibited adenocarcinoma features and expressed epithelial and metabolic markers resembling human ovarian cancer. Although DMBA-induced cancer models are not exact replicas of the human body, striking histological similarities have been found between rat ovarian carcinomas and human serous and endometrioid tumor types (Nishida et al. 1998).

The results of this study showed that there were significant differences between liver and kidney function in normal rats compared with rats treated with DMBA. DMBA is an immune suppressor and potent pro-carcinogen agent. DMBA induces the formation of free radicals such as ROS, superoxide anions, and intracellular hydroxyl radicals, causing lipid peroxidation that alters cellular and subcellular conditions, resulting in DNA damage, disrupting tissue redox balance, and interfering with various biochemical pathways. Oxidative stress from ROS formation can affect vital organs such as the liver and kidneys. The kidneys are organs that cannot escape the toxic effects of DMBA, given their role in active metabolism and receiving a quarter of the cardiac output. The kidneys also function as filtration and excretion organs for various metabolic waste substances, making them sites of accumulation for toxic substances, especially DMBA. DMBA exposure causes histological changes in the kidneys, leading to dilation and disintegration of the kidney tubules, especially in the epithelial cells of the proximal convoluted tubules and Bowman's capsules, which are highly sensitive to DMBA toxicity (Dosumu et al. 2021).

Similarly, the liver is the main organ responsible for metabolizing various chemical compounds where chemical carcinogens are metabolically stored and activated. DMBA exposure can lead to liver dysfunction characterized by elevated AST, ALT, ALP, and total serum bilirubin (Akhouri et al. 2020). This study did not find clinically significant differences in liver and kidney function between the DMBA and sham groups. It was indicated that liver and kidney function remain intact in the 28-week-old DMBA-induced Wistar rat model due to the absence of systemic toxicity, suggesting that DMBA induction in one month has not yet exhibited systemic toxicity.

Conclusion

In conclusion, at the 28 weeks of observation, all parameters measured in the study showed a significant value than the sham group. Therefore, it was concluded that silk-implanted DMBA treatments in the present study are capable of causing ovarian tumors in rats, specifically ovarian serous carcinoma, as well as tumor metastases to adjacent and distant organs. This model closely resembles the morphology of ovarian serous carcinoma in humans. As a result, this technique can help us better understand ovarian cancer's pathophysiology and develop new therapeutic strategies.

Acknowledgment

The authors thank CV Mega Utama Medika and IratCo Laboratory for their support during the research.

Conflict of interest

The authors declare no conflict of interest.

Authors' Contribution

FVD, WA, DN, An, HW, PEW, and VJ designed the protocol and wrote the manuscript. FVD, WA, DN, VJ, PEW, RTP, and CBR performed experiments, interpreted the results of the experiments, and conducted data analysis. All authors approved the final version of the manuscript.

REFERENCES

Akhouri V, Kumari M and Kumar A, 2020. Therapeutic effect of Aegle marmelos fruit extract against DMBA induced breast cancer in rats. Scientific Reports 10(1): 18016. https://doi.org/10.1038/s41598-020-72935-2

Anisimov VN, Ukraintseva SV and Yashin AI, 2005. Cancer in rodents: does it tell us about cancer in humans? Nature Reviews. Cancer 5(10): 807-819. https://doi.org/10.1038/nrc1715

Barbolina MV, 2018. Molecular Mechanisms Regulating Organ-Specific Metastases in Epithelial Ovarian Carcinoma. Cancers 10(11). https://doi.org/10.3390/cancers10110444

Berek JS, Renz M, Kehoe S, Kumar L and Friedlander M, 2021. Cancer of the ovary, fallopian tube, and peritoneum: 2021 update. International Journal of Gynaecology and Obstetrics 155(Suppl 1): 61-85. https://doi.org/10.1002/ijgo.13878

Campbell S and Gentry-Maharaj A, 2018. The role of transvaginal ultrasound in screening for ovarian cancer. Climacteric 21(3): 221-226. https://doi.org/10.1080/13697137.2018.1433656

Cho KR and Shih Ie M, 2009. Ovarian cancer. Annual Review of Pathology 4: 287-313. https://doi.org/10.1146/annurev.pathol.4.110807.092246

Crist KA, Zhang Z, You M, Gunning WT, Conran PB, Steele VE and Lubet RA, 2005. Characterization of rat ovarian adenocarcinomas developed in response to direct instillation of 7,12-dimethylbenz[a]anthracene (DMBA) coated suture. Carcinogenesis 26(5): 951-957. https://doi.org/10.1093/carcin/bgi039

Dosumu O, Bababode A, Rotimi S, Akamo J, Omotosho O, Sani L, Osinuga K, Taiwo O, Owolabi O and Ojo O, 2021. DMBA-Induced Kidney Dysfunction: Effects of Supplementary Dietary Vitamin K in Rats. Tropical Journal of Natural Product Research 5: 917-923. https://doi.org/10.26538/tjnpr/v5i5.19

Eisenhauer EL, Salani R and Copeland LJ, 2018. Epithelial Ovarian Cancer. In: Clinical Gynecologic Oncology (pp. 253-289.e214).

Gui P and Bivona TG, 2022. Evolution of metastasis: new tools and insights. Trends in Cancer 8(2): 98-109. https://doi.org/10.1016/j.trecan.2021.11.002

Hibbs K, Skubitz KM, Pambuccian SE, Casey RC, Burleson KM, Oegema TR, Jr., Thiele JJ, Grindle SM, Bliss RL and Skubitz AP, 2004. Differential gene expression in ovarian carcinoma: identification of potential biomarkers. The American Journal of Pathology 165(2): 397-414. https://doi.org/10.1016/s0002-9440(10)63306-8

Huang Y, Jiang W, Wang Y, Zheng Y, Cong Q and Xu C, 2012. Enhanced efficacy and specificity of epithelial ovarian carcinogenesis by embedding a DMBA-coated cloth strip in the ovary of rat. Journal of Ovarian Research 5(1): 21. https://doi.org/10.1186/1757-2215-5-21

Israeli O, Gotlieb WH, Friedman E, Korach J, Friedman E, Goldman B, Zeltser A, Ben-Baruch G, Rienstein S and Aviram-Goldring A, 2004. Genomic analyses of primary and metastatic serous epithelial ovarian cancer. Cancer Genetics and Cytogenetics 154(1): 16-21. https://doi.org/10.1016/j.cancergencyto.2004.02.006

Lengyel E, 2010. Ovarian cancer development and metastasis. The American Journal of Pathology 177(3): 1053-1064. https://doi.org/10.2353/ajpath.2010.100105

Louisa M, 2019. Hewan Model Kanker Ovarium untuk Studi Preklinik dan Pengembangan Obat Kanker Ovarium Jurnal Ilmu Kefarmasian Indonesia 17(2): 139-149

Mccormick DL, 2017. Chapter 12 - Preclinical Evaluation of Carcinogenicity Using Standard-Bred and Genetically Engineered Rodent Models. In A. S. Faqi (Ed.), A Comprehensive Guide to Toxicology in Nonclinical Drug Development (2nd Ed) (pp. 273-292). Boston: Academic Press.

Mcdermott SP, Ranheim EA, Leatherberry VS, Khwaja SS, Klos KS and Alexandercm, 2007. Juvenile syndecan-1 null mice are protected from carcinogen-induced tumor development. Oncogene 26(10): 1407-1416. https://doi.org/10.1038/sj.onc.1209930

Nishida T, Sugiyama T, Kataoka A, Ushijima K and Yakushiji M, 1998. Histologic characterization of rat ovarian carcinoma induced by intraovarian insertion of a 7,12-dimethylbenz[a]anthracene-coated suture: common epithelial tumors of the ovary in rats? Cancer 83(5): 965-970. https://doi.org/10.1002/(sici)1097-0142(19980901)83:5<965::aid-cncr23>3.0.co;2-s

Rämer PC, Chijioke O, Meixlsperger S, Leung CS and Münz C, 2011. Mice with human immune system components as in vivo models for infections with human pathogens. Immunology and Cell Biology 89(3): 408-416. https://doi.org/10.1038/icb.2010.151

Rengarajan T, Rajendran P, Nandakumar N, Lokeshkumar B, Rajendran P and Nishigaki I, 2015. Exposure to polycyclic aromatic hydrocarbons with special focus on cancer. Asian Pacific Journal of Tropical Biomedicine 5(3): 182-189. https://doi.org/10.1016/S2221-1691(15)30003-4

Sandhiutami N, Arozal W, Louisa M, Rahmat D, Wuyung P and Fakhrul Ulum M, 2019. Induction of Epithelial Ovarian Cancer by Implantation of 7,12-dimethylbenz(a)athracene (DMBA) Coated Silk in Rats. Journal of Young Pharmacists 11: 56-61. https://doi.org/10.5530/jyp.2019.11.12

Souza BRD, Oliveira G, Leme G, Cabral FaT, Reis IB, Felizzola CR, Duran N, Fávaro WJ and Anglesio M, 2023. A DMBA-induced ovarian cancer model: Could it be clinically useful to test OncoTherad and erythropoietin as anticancer approaches? 41(16_suppl): e17589-e17589. https://doi.org/10.1200/JCO.2023.41.16_suppl.e17589

Sung H, Ferlay J, Siegel RL, Laversanne M, Soerjomataram I, Jemal A and Bray F, 2021. Global Cancer Statistics 2020: GLOBOCAN Estimates of Incidence and Mortality Worldwide for 36 Cancers in 185 Countries. CA: a Cancer Journal for Clinicians 71(3): 209-249. https://doi.org/10.3322/caac.21660

Tan DS, Agarwal R and Kaye SB, 2006. Mechanisms of transcoelomic metastasis in ovarian cancer. The Lancet. Oncology 7(11): 925-934. https://doi.org/10.1016/s1470-2045(06)70939-1

Taylor I and Mowat V, 2020. Comparison of longevity and common tumor profiles between Sprague-Dawley and Han Wistar rats. Journal of Toxicologic Pathology 33(3): 189-196. https://doi.org/10.1293/tox.2020-0005

Tunca JC, Ertürk E, Ertürk E and Bryan GT, 1985. Chemical induction of ovarian tumors in rats. Gynecologic Oncology 21(1): 54-64. https://doi.org/10.1016/0090-8258(85)90232-x

Vanderhyden BC, Shaw TJ and Ethier JF, 2003. Animal models of ovarian cancer. Reproductive Biology and Endocrinology : RB&E 1: 67. https://doi.org/10.1186/1477-7827-1-67

Wang Y, Zhang Z, Lu Y, Yao R, Jia D, Wen W, Laregina M, Crist K, Lubet R and You M, 2008. Enhanced susceptibility to chemical induction of ovarian tumors in mice with a germ line p53 mutation. Molecular Cancer Research 6(1): 99-109. https://doi.org/10.1158/1541-7786.Mcr-07-0216